Published in final edited form as:
Cancer Res. 2012 April 15; 72(8): 1964–1974. doi:10.1158/0008-5472.CAN-11-3208.

Densely Granulated Murine NK Cells Eradicate Large Solid Tumors

Rebecca B. Liu[1,2,*], **Boris Engels**[2,*], **Ainhoa Arina**[2], **Karin Schreiber**[2], **Elizabeth Hyjek**[2], **Andrea Schietinger**[2], **David C. Binder**[3], **Eric Butz**[5], **Thomas Krausz**[2], **Donald A. Rowley**[2], **Bana Jabri**[4], and **Hans Schreiber**[2]

[1]Committee on Immunology, The University of Chicago, Chicago, IL 60637

[2]Department of Pathology, The University of Chicago, Chicago, IL 60637

[3]Committee on Cancer Biology, The University of Chicago, Chicago, IL 60637

[4]Department of Medicine, The University of Chicago, Chicago, IL 60637

[5]Inflammation Department, AMGEN, Seattle, WA 98119

Abstract

NK cells inhibit early stages of tumor formation, recurrence and metastasis. Here we show that NK cells can also eradicate large solid tumors. Eradication depended on the massive infiltration of proliferating NK cells due to IL15 released and presented by the cancer cells in the tumor microenvironment. Infiltrating NK cells had the striking morphological feature of being densely loaded with PAS-positive, diastase-resistant granules, resembling uterine NK cells. Perforin-mediated killing by these densely granulated NK cells was essential for tumor eradication. Expression of the IL15 receptor α on cancer cells was needed to efficiently induce granulated NK cells and expression on host stromal cells was essential to prevent tumor relapse after near complete destruction. These results indicate that IL15 released at the cancer site induces highly activated NK cells that lead to eradication of large solid tumors.

Keywords

Tumor eradication; NK cells; IL15; tumor margin; perforin

Introduction

Natural killer (NK) cells were originally discovered as peripheral blood lymphocytes that killed certain cancer cells *in vitro* (1–4). *In vivo*, NK cells inhibited primary tumor formation, tumor recurrence and metastasis, but usually only at incipient stages (for review see (5)). In patients, intratumoral NK cells may reduce metastatic seeding thereby leading to longer survival (6). Transformed cells often have decreased MHC class I surface expression or have induced expression of ligands for activating receptors on NK cells (7, 8), and thus are targets of NK cells and their receptors. However, the lack of studies showing NK cells

Corresponding Author: Hans Schreiber, The University of Chicago, Department of Pathology, Room G-304, MC 3008, 5841 South Maryland Avenue, Chicago, IL 60637-5420, Phone: (773) 702-9204, Fax: (773) 702-9224, hszz@uchicago.edu.
*These authors equally contributed to this work
Present affiliation for A.S. is Department of Immunology, University of Washington, Seattle, WA 98195.

E.B. is employed by Amgen Inc., all other authors declare no conflict of interest.

eliminating established solid tumors has cast doubts on the clinical usefulness of NK cells in the therapy of advanced solid tumors.

NK cells can be activated with high doses of IL-2 to proliferate and kill a broad panel of cancer targets and this is being exploited clinically in selected groups of cancer patients (9–11); while adoptive transfer of NK cells activated *in vitro* with IL-2 failed to cause tumor regression in melanoma patients (12). IL15, discovered in 1994 (13), also activates human NK cells to kill cancer cells via components of the IL-2 receptor by a perforin-dependent mechanism (14, 15). In mice, IL15 is required for the development and survival of NK cells, and these IL15 effects depend on expression of the IL15 receptor α (IL15Rα) on cells other than the NK cell (16). Similar to IL2-induced NK cells, IL15-induced cells also can prevent cancer development and metastasis (17–19). In addition to activating NK cells, IL15 also activates T cells and thereby induces certain T cell-mediated anti-cancer responses (for review see (20)). Nevertheless, whether IL15 was expressed as a transgene by the cancer cells (21–24) or given as treatment (25–28), anti-cancer effects remained limited to the prevention of cancer development and metastasis or reduced tumor growth. Therefore, it certainly has remained unclear whether NK cells, when properly activated by IL15, could have an effect on solid tumors once grown to clinically relevant sizes. Here we show that, even in the complete absence of T cell immunity, NK cells can be induced to eradicate large solid tumors.

Materials and Methods

Mice

Perforin-deficient (Jackson Laboratory) and IL15Rα-deficient mice (provided by A. Ma, University of California, San Francisco, CA) were crossed to *Rag1*$^{-/-}$ mice (Jackson Laboratories) and *Rag2*$^{-/-}$ $\gamma c^{-/-}$ (Taconic, Hudson, NY), C3H/HeN (Charles River Laboratories, Wilmington, MA), and IL15-transgenic mice (DQ8-D^{d}-IL-15, (29)) were maintained under specific pathogen-free conditions at the University of Chicago facilities. The IACUC at the University of Chicago approved all animal experiments.

Cells

All cells were cultured in DMEM, 5% FCS. P. Ohashi (University of Toronto, Canada) with permission of H. Hengartner (University Hospital, Switzerland) provided the MC57G fibrosarcoma cell line. 8215 is a MCA-induced cancer line generated in an IL15Rα-deficient mouse (125μg MCA). 9604 is a UV-induced cancer line of a K$^{b-/-}$D$^{b-/-}$ mouse (30) (3 UV exposures/week for half a year; mice provided by A. Chervonsky, The University of Chicago, IL). Both are primary lines that have never been passaged in a mouse. The spontaneous line AG104A of C3H/HeN origin was described (31). All cell lines were passaged only a few times (less than 1 month) after thawing of working-batch freezings, which were generated shortly after obtaining cell lines, to reduce total number of passages to a minimum. Cell lines were authenticated by morphology and growth rate and were Mycoplasma-free.

To transduce the 4 cell lines, we used MFG-IL15HS-IRES-ECFP, MFG-IL15Rα or the empty amphotropic virus. Cultures were flow sorted to enrich for positive cells (see Supplementary Materials and Methods for plasmids and details).

ELISA and Flow cytometry

M-IL15 or M-control cells were plated at 4×10^4 cells/mL in a T25 culture flask. 48h supernatants were assayed using the mouse IL15 Ready-SET-Go! kit (eBioscience).

Single cell suspensions from mouse tissue or trypsinized MC57 cells were first blocked with anti-CD16/anti-CD32 antibody then stained with conjugated antibodies (see Supplementary Materials and Methods for antibodies). FACS data were collected on a FACSCalibur or LSRII, and sorting was performed on a FACS Aria (all BD Biosciences) and analyzed using FlowJo software (Treestar Inc., Ashland, OR).

Tumor challenges, measurements and reisolations

Mice were injected subcutaneously with $2.5–5\times10^6$ cells in 100μL of PBS, unless indicated otherwise. Tumor volume was measured every 2–5 days with calipers along three orthogonal axes and calculated by abc/2. Statistical significance of tumor eradication was determined by the Fisher Exact Probability Test.

Anti-IL15 (clone M96, provided by Amgen, Seattle, WA) was injected once at 45μg pre cancer cell inoculation and 95μg weekly thereafter. To deplete NK cells, mice received 100μg anti-NK1.1 (clone PK136) every 3–4 days; NK cell depletion was confirmed by flow cytometry of peripheral blood samples with anti-NK1.1 and anti-CD122. For bone marrow transfers, 3×10^7 cells were injected into each recipient mouse. Details are found in Supplementary Materials and Methods.

Microscopy

Images were taken on the Leitz Laborlux D microscope with a Leitz 63×/1.4 objective and Zeiss 20×/0.25 and 6.3×/0.16 objectives using the QImaging Retiga 2000R camera and QCapture software. Macroscopic images were taken using the Nikon Coolpix 6000 camera.

Histology and Immunohistochemistry

Tissue was frozen in OCT using isopentane in dry ice. 4μm sections were cut, dried, mounted and fixed in acetone. Prior to staining, endogenous peroxidase was blocked (Dako dual endogenous enzyme block, Carpinteria, CA). Anti-NK1.1-FITC and anti-granzyme B-FITC were used at 1μg/mL and 2.5μg/mL, respectively. Anti-FITC (Pierce) was used as recommended by the manufacturers. Horseradish peroxidase was developed using DAB (Dako) for 10min. Slides were counterstained with hematoxylin, dehydrated in alcohols and mounted in mounting medium (Sakura Finetek, USA, Torrance, CA). Details are found in Supplementary Materials and Methods.

Results

IL15 secreting cancer cells form large tumors in mice lacking NK and T cells

MC57 fibrosarcoma cells were transduced with the murine IL15 gene preceded by the IL-2 leader sequence; levels of ECFP fluorescence were used for selecting cells secreting large amounts of IL15 (M-IL15) (Fig. 1A, Fig. S1). As control, MC57 cells were transduced with the empty ECFP vector (M-control). M-IL15 cells did not form tumors in *Rag1*$^{-/-}$ mice (Fig. 1B, left). However, M-IL15 and M-control cells grew at similar rates and formed large tumors in *Rag2*$^{-/-}$ $\gamma c^{-/-}$ mice (Fig. 1B, middle), which are unable to respond to IL15. Tumors also grew in *Rag1*$^{-/-}$ mice while these were given a neutralizing anti-IL15 antibody (Fig. 1B, right panel). Figure 1C shows that peripheral NK cells were absent in both types of mice in which M-IL15 grew.

Large solid tumors regress after anti-IL15 application is stopped

Surprisingly, large M-IL15 tumors (>1cm in diameter or >500mm^3 in volume, Fig. 1B) were rejected completely after withdrawal of the anti-IL15 antibody (Fig. 1D, left; Table SI). By contrast, most M-control tumors continued to grow at the same rate. Regression of large

IL15-secreting tumors did not stop the growth of contralateral M-control tumors suggesting that the effect of IL15 is largely restricted to the local microenvironment of the IL15-secreting tumor (Fig. 1D, middle).

Densely granulated cells found in the regressing tumor

M-control tumors growing in anti-IL15 treated *Rag1*$^{-/-}$ mice were densely packed with viable cancer cells, many in mitosis; only the center of these M-control tumors was necrotic (Fig. 2A). Cross-sections of regressing M-IL15 tumors 12 days after final injection of anti-IL15 showed mostly necrotic tumor tissue (Fig. 2B). The few partially viable areas were packed with densely granulated cells and it was difficult to identify any remaining viable cancer cells. The granules stained bright magenta with periodic acid-Schiff (PAS) and were resistant to pretreatment with diastase. Some of these granulated cells in the regressing tumors were undergoing mitosis suggesting that the granulated cells represented infiltrating host cells rather than thanatosomes derived of dying cancer cells (32) (Fig. 2B right, arrow; Fig.5, left middle).

Transfer of *Rag1*$^{-/-}$ bone marrow cells causes regression of M-IL15 tumors in *Rag2*$^{-/-}$ *γc*$^{-/-}$ mice

Rag2$^{-/-}$ *γc*$^{-/-}$ mice reconstituted with *Rag1*$^{-/-}$ bone marrow were resistant to outgrowth of M-IL15 cancer cells (Fig. 3A). Next we treated *Rag2*$^{-/-}$ *γc*$^{-/-}$ mice bearing M-control or M-IL15 tumors with bone marrow from *Rag1*$^{-/-}$ mice 2 weeks after cancer cell inoculation (tumor volumes between 200 and 500mm^3). While the bone marrow transfer had no apparent influence on the growth of the M-control tumors, the bone marrow derived cells eradicated M-IL15 tumors in 50% of the mice (Fig. 3B), suggesting that γc$^+$ bone marrow-derived cells can reject established tumors. As observed in M-IL15 tumors after anti-IL15 treatment was stopped, numerous cells filled with PAS$^+$ diastase-resistant granules were found in the tumors (Fig. 3C). These cells were absent in the tumors prior to the bone marrow transfer. Adoptive transfers of spleen cells from *Rag1*$^{-/-}$ mice also had an effect on M-IL15 but not M-control tumors, which was however not as strong as seen for bone marrow transfers (data not shown).

Densely granulated NK1.1$^+$ cells are essential for tumor eradication

Immunohistochemical analyses showed that the majority of tumor-infiltrating cells in regressing tumors expressed NK1.1 and granzyme B (Fig. 4A). To confirm that the densely granular cells found in the regressing tumors were tumor-infiltrating NK cells, we sorted NK1.1$^+$ cells also expressing DBA, a marker of densely granular uterine NK (uNK) cells, from M-IL15 tumors and prepared cytospins. Although some of the granules seemed to have collapsed or been extruded during the isolation process, the reisolated and sorted NK1.1$^+$DBA$^+$ cells were packed with PAS$^+$ granules (Fig 4B). To determine whether NK cells were indeed required for the rejection of the M-IL15 tumors, we depleted NK cells from anti-IL15-treated *Rag1*$^{-/-}$ mice after withdrawal of the antibody. In accordance with our hypothesis, we found that in the absence of NK cells, tumors expressing IL15 were not rejected (Fig. 4C, Table SI). Flow cytometry revealed that the tumor-infiltrating NK cells expressed normal levels of NKp46, 2B4 and CD122 but reduced levels of DX5 and NKG2D, compared with splenic NK cells (Fig. 4D); differences in marker expression were not due to differences in sample preparation (data not shown). The infiltrating NK cells also had decreased CD27, an immature NK cell marker, and increased 4-1BB, CD11b and TRAIL expression, characteristic of activated NK cells (33, 34). Despite the similarities to activated NK cells, we found no PAS$^+$ NK cells in spleens from poly I:C activated wild-type mice (data not shown), nor in short-term cultures of NK cells activated with IL15 (Fig S2A). Also, mice with heavily infiltrated M-IL15 tumors had only very few granulated NK cells in their spleens (Fig S2B). Microscopic analysis from serial sacrifices showed that the NK cells

took time to mature into granular PAS^+ cells and could not be detected in tumors as early as 3 days post cancer cell injection but were present by day 12 (Fig. S3).

An analysis of cytokines that may have synergized with IL15 to promote the differentiation of densely granular NK cells was conducted. $CD11b^+$ stromal cells in growing M-IL15 tumors expressed IL12 and IL10, but no detectable IL18 and TGF-β (Fig. S4). Cancer cells obtained from growing tumors or cultured *in vitro* did not express any of these cytokines at detectable levels (Fig. S4 and data not shown, respectively).

Eradication depends on perforin released by infiltrating NK cells and destruction of cancer cells at the tumor margin

Given the prominent granules found in M-IL15 tumors, we hypothesized that perforin was involved in tumor rejection. We evaluated the rejection of M-IL15 tumors grown in $Rag1^{-/-}Prf1^{-/-}$ mice with anti-IL15 antibody after antibody treatment was stopped. Indeed, in the absence of perforin, we found M-IL15 tumors grew with similar kinetics to viable M-control tumors (compare left with right panel of Fig. 1D; Table SI). Surprisingly, the tumors growing in $Rag1^{-/-}Prf1^{-/-}$ mice were mostly necrotic (Fig. 5 left; Fig S3 for non-anti-IL15 treated $Rag1^{-/-}Prf1^{-/-}$ mice). Control tumors only displayed a small area of necrosis typical for fast growing tumors (Fig 2A). The rim of M-IL15 tumors in $Rag1^{-/-}Prf1^{-/-}$ mice was heavily infiltrated with densely granulated proliferating NK cells intermingled with proliferating cancer cells.

We also analyzed the appearance of M-IL15 tumors growing in $Rag1^{-/-}$ mice shortly after cessation of anti-IL15 treatment (Fig. 5, right panels), when the tumor had not yet begun to shrink and no NK cells were detectable in the peripheral blood. The margins of the tumors lacked PAS^+ cells but contained dividing cancer cells, while further inside the tumor, there was heavy infiltration of PAS^+ cells and cancer cell destruction. The center remained vascularized, however, which contrasts to the center of the tumor in the $Rag1^{-/-}Prf1^{-/-}$ mouse where no tumor vessels were detected. This indicated that the anti-IL15 antibody exerted its neutralizing activity mostly at the tumor margin and that this effect was sufficient to allow tumor growth.

Stromal IL15Rα expression is not required for temporary regression but is required for tumor eradication

Unlike most cytokines, IL15 is presented *in trans* on IL15Rα expressing cells. MC57 cells express high levels of IL15Rα (Fig. 6A) and thus can present IL15 to NK cells. To determine whether IL15Rα expression by cancer cells and not the stroma was sufficient for tumor rejection, we grew M-IL15 cells in $Rag1^{-/-}IL15R\alpha^{-/-}$ mice. Although $Rag1^{-/-}IL15R\alpha^{-/-}$ mice are initially deficient in NK cells, M-IL15 tumors decreased in size after cessation of anti-IL15 treatment (Fig. 6B). Similarly, when $Rag1^{-/-}IL15R\alpha^{-/-}$ mice were injected with M-IL15 cancer cells without being pretreated with anti-IL15 antibody, tumors initially grew and then regressed almost completely. However, most tumors eventually relapsed, except for one (Fig. 6B, Table S1). Analysis of $Rag1^{-/-}IL15R\alpha^{-/-}$ mice bearing M-IL15 tumors showed that NK cells can be found in the peripheral blood early but not later, when tumors began to relapse (Fig. 6C). Taken together, IL15Rα expression seems to be required on stromal cells in order to achieve complete tumor eradication.

A mixture containing 5% of non-IL15-secreting cancer cells never formed tumors (Fig. S5A). With higher numbers of non-secreting cancer cells (10–20% of cancer cells) there was outgrowth of tumors, probably due to no sufficient IL15 to be trans-presented on IL15Rα of non-secreting cancer and stromal cells, resulting in the incapability of NK cells to kill. As

demonstrated by the selection of non-secreting cells (Fig S5B), all IL15-secreting cells were specifically deleted.

Several cancer cell lines induce densely granulated NK cells

We transduced three other cancer cell lines to express IL15 and/or IL15Rα at high levels (Fig. S6). Both cancer lines expressing IL15 and Rα, C3H/HeN-derived AG104A-IL15-Rα and C57BL/6-derived 9604-IL15-Rα formed viable tumors when injected in syngeneic mice pretreated with anti-IL15 antibody. Histology of tumors from non-treated animals showed destruction of cancer cells and infiltration by densely granulated NK cells (Fig. 7A and B).

The IL15Rα-deficient cancer line 8215 was transduced to express IL15 only (Fig. S6). This line also formed viable tumors in *Rag1*$^{-/-}$*Prf1*$^{-/-}$ mice (Fig. 7C). In contrast to M-IL15 tumors growing in *Rag1*$^{-/-}$*Prf1*$^{-/-}$ mice, these tumors did not show extensive central necrosis and infiltration of only very few granular NK cells. Taken together, densely granular NK cells are induced in different cancer lines expressing both high levels of IL15Rα and of secreted IL15. IL15Rα is needed on cancer cells to efficiently induce densely granulated NK cells.

Discussion

We show that IL15-induced NK cells can eliminate large established solid tumors in a host completely devoid of T and B cells. This unprecedented effect was apparently caused by massive influx of a unique type of very densely granulated NK cells that resemble a NK subtype described in the mammalian uterus during pregnancy (uNK) (35) that also depends on IL15 (36). Unlike granulocytes, which are end-stage cells, these heavily granulated NK cells were still clearly proliferating at the tumor site. Other mature NK cells can also undergo blastogenesis such as virally induced NK cells in the spleen (37) and uNK cells in the uterus (38). As described for mature uNK cells, the granules of the IL15-induced NK cells in the tumor tissue were PAS-positive and diastase-resistant and their cytoplasmic membrane stained with the lectin Dolichos biflorus agglutinin (DBA), which binds to glycoconjugates containing N-acetyl-D-galactosamine. However, it may be inappropriate to draw further analogies between the densely granulated NK cells described here and uNK because the tumor infiltrating IL15-induced NK cells are a cytolytic population generated by manipulating the tumor microenvironment. Also, while perforin is required for the eradication of tumors by these granulated NK cells, uNK do not need perforin for successful pregnancies (39).

Transgenic mice overexpressing secreted IL15 do not show densely granulated NK cells in their spleen, liver or gut (data not shown), nor do short-term cultures of wild-type or IL15-transgenic splenic NK cells stimulated with high-dose IL15. The difference to IL15-secreting tumors might be the level of IL15 secretion and/or IL15Rα expression, but also the presence of other cytokines. IL12 was shown to increase the production of NK effector cytokines and IFN-γ while it suppressed target killing (40, 41). IL10, in contrast, was recently shown to enhance cytolytic activity of NK cells (42). High local levels of IL15 were, nevertheless, critical for the generation of densely granulated NK cells; cancer lines not expressing IL15 induced only very few granulated cells (Fig S2C). Furthermore, expression of IL15Rα by cancer cells was needed for effective induction of PAS^{+} cells. Finally, infiltration of granulated NK cells required time. Taken together, a specific tumor milieu with high IL15 and IL15Rα expression and several days of maturation were needed for the differentiation of densely granulated NK cells with anti-tumor function.

We have several lines of experiments indicating that these IL15-induced densely granulated NK cells were indeed the effectors eradicating the large tumors: (i) tumors formed in mice

deficient in NK cells such as *Rag2*$^{-/-}$ $\gamma c^{-/-}$ mice and *Rag1*$^{-/-}$ mice given anti-IL15 antibody to deplete NK cells but not in *Rag1*$^{-/-}$ mice that contain NK cells; (ii) transfer of bone marrow or spleen cells from *Rag1*$^{-/-}$ mice into tumor-bearing *Rag2*$^{-/-}$ $\gamma c^{-/-}$ or cessation of NK depletion with anti-IL15 led to tumor rejection accompanied with tumor infiltration of these heavily granulated cells; (iii) cells isolated from the tumors had characteristic peripheral NK markers when stained by immunohistochemistry or analyzed by flow cytometry; (iv) infiltrating cells sorted for NK1.1 and DBA showed PAS^{+} granules in cytospins; (v) only IL15-secreting but not contralateral non-secreting control tumors were eradicated; (vi) the anti-NK1.1 antibody administration abolished rejection; (vii) densely granulated NK cells were completely absent from the tumor margin during systemic application of anti-IL15 antibody.

Several methodological differences to other studies expressing IL15 in cancer cells could explain why such strong anti-tumor effects have not been described earlier. For example, earlier studies used human IL15, which was not fused to any signaling peptide needed for effective secretion; comparison of ELISA data suggests a up to 7000-fold higher secretion of IL15 (22). Furthermore, it is not clear whether the cancers expressed IL15Rα. More recent studies employing highly secreted IL15 do show NK-dependent inhibition of tumor outgrowth, similar to what we find; whether rejection of established tumors was studied in these models has not been described (17, 18, 24). We were able to study rejection of established tumors by growing them under protection of anti-IL15 antibody, as trans-presented IL15 is needed for (i) augmenting susceptibility to killing (18) and (ii) survival of circulating NK cells. Interestingly, NK cells survived in the center of tumors growing in anti-IL15-treated mice, consistent with the notion that antibodies cannot effectively diffuse into solid tumors (43). The rim of these tumors remained NK cell-free and viable, even shortly after cessation of the antibody treatment. Tumors began to regress approximately 10 days after the last dose of antibody when circulating and infiltrating NK cells were detected. It remains unclear whether these NK cells originated from the surviving NK cells within the tumor or whether they infiltrated from the periphery and matured in the tumor.

Tumors in mice lacking perforin had vast central necrosis while the rim remained viable. It is tempting to speculate that the destruction of the greater mass of the tumor was caused by IFN-γ and TNF still being produced by the perforin-deficient IL15-induced NK cells, as IFN-γ was shown to be an important effector molecule in adoptively transferred NK cells (44). Furthermore, infiltrated NK cells had upregulated 4-1BB, which has been implicated with elevated IFN-γ secretion (45). Although likely, it needs to be confirmed that NK cells caused the central necrosis in *Prf*$^{-/-}$ mice and the effector molecules involved need to be defined. Nevertheless, massive central necrosis and dense infiltration by perforin-deficient NK cells at the tumor margin did not change the growth rate of the cancer. The similarly growing IL15-secreting tumors in perforin-competent mice receiving anti-IL15 antibody looked histologically different, but also showed central necrosis and a viable tumor rim. These results indicate that the viability of the margins of tumors, not of the bulk tumor beneath this layer, determine whether eradication occurs.

Interestingly, tumors relapsed after nearly complete destruction when the hosts lacked IL15Rα. As discussed for cancer cells above, the tumor stroma may need to express IL15Rα to become a target for NK cells and killing of stroma may be needed for complete eradication (46). Since IL15Rα expression on non-NK cells is required for maturation of NK cells from precursors (16), IL15Rα expression on cancer cells growing in the IL15Rα-deficient hosts must have sufficed for developing and maintaining fully mature NK cells from precursors. The existence of such precursors has previously been reported (for review see (47)). However, after the NK cells have killed the cancer cells, this support was

obviously eliminated. Accordingly, relapse of IL15-secreting tumors in IL15Rα–deficient hosts correlated with the absence of peripheral NK cells.

Now the greatest challenge for utilizing IL15 in cancer therapeutics is targeting the malignant tissue. Based on the combined findings, we think IL15 and IL15Rα must be localized to the tumor. Localizing IL15 to the tumor is daunting but ongoing research suggests that linking IL15 and its stabilizing IL15Rα (25–28) to a tumor-specific antibody could be an effective approach. While this strategy eliminates the appeal of NK cells in not requiring identification of antigens, it aims to take advantage of the unprecedented destructive ability of IL15-activated NK cells for large established tumors. Kroemer *et al.* showed that soluble IL15/IL15Rα conjugates could stimulate NK cells *in vivo* to reject skin allo-grafts in the absence of adaptive immune cells (48). Once a proper delivery approach is developed, these effector NK cells need to be induced only in the microenvironment of the tumor margin sparing the rest of the body from the side effects and suffering that accompany many available therapies today.

Supplementary Material

Refer to Web version on PubMed Central for supplementary material.

Acknowledgments

We thank Michael Caligiuri for reagents and Jennifer Stone and David Kranz for technical support and discussions. We thank Mark Smyth and Laurence Zitvogel for advice on phenotypic analysis and Sigrid Dubois, Nicole Fortenbery, Patricia González-Greciano, Jose Moyano, Vinay Kumar, and David Raulet for helpful suggestions. Finally, we thank the staff of the University of Chicago Flow Cytometry Core Facility and Elsamma Chettiath, Cezary Ciszewski, Dorothy Kane, and Christy Schmehl for technical assistance.

Grant support

This research was supported by NIH Grants P01-CA97296, R01-CA22677 and R01-CA37516 to H.S and the University of Chicago Committee on Immunology training grant (T32 AI 0709) to R.B.L..

References

1. Kiessling R, Klein E, Wigzell H. "Natural" killer cells in the mouse. I. Cytotoxic cells with specificity for mouse Moloney leukemia cells. Specificity and distribution according to genotype. Eur J Immunol. 1975; 5:112–117. [PubMed: 1234049]
2. Herberman RB, Nunn ME, Lavrin DH. Natural cytotoxic reactivity of mouse lymphoid cells against syngeneic and allogeneic tumors. I. Distribution of reactivity and specificity. Intl J Cancer. 1975; 16:216–229.
3. Sendo F, Aoki T, Boyse EA, Buafo CK. Natural occurrence of lymphocytes showing cytotoxic activity to BALB/c radiation-induced leukemia RL male 1 cells. J Natl Cancer Inst. 1975; 55:603–609. [PubMed: 1159837]
4. Joihdal M, Press H. Surface markers on human B and T lymphocytes VI. Cytotoxicity against cell lines as a functional marker for lymphocyte subpopulations. Int J Cancer. 1975; 15:596. [PubMed: 806545]
5. Terme M, Ullrich E, Delahaye NF, Chaput N, Zitvogel L. Natural killer cell-directed therapies: moving from unexpected results to successful strategies. Nat Immunol. 2008; 9:486–494. [PubMed: 18425105]
6. Coca S, Perez-Piqueras J, Martinez D, Colmenarejo A, Saez MA, Vallejo C, et al. The prognostic significance of intratumoral natural killer cells in patients with colorectal carcinoma. Cancer. 1997; 79:2320–2328. [PubMed: 9191519]
7. Gasser S, Orsulic S, Brown EJ, Raulet DH. The DNA damage pathway regulates innate immune system ligands of the NKG2D receptor. Nature. 2005; 436:1186–1190. [PubMed: 15995699]

8. Guerra N, Tan YX, Joncker NT, Choy A, Gallardo F, Xiong N, et al. NKG2D-deficient mice are defective in tumor surveillance in models of spontaneous malignancy. Immunity. 2008; 28:571–580. [PubMed: 18394936]
9. Grimm EA, Mazumder A, Zhang HZ, Rosenberg SA. Lymphokine-activated killer cell phenomenon. Lysis of natural killer-resistant fresh solid tumor cells by interleukin 2-activated autologous human peripheral blood lymphocytes. J Exp Med. 1982; 155:1823–1841. [PubMed: 6176669]
10. Trinchieri G, Matsumoto-Kobayashi M, Clark SC, Seehra J, London L, Perussia B. Response of resting human peripheral blood natural killer cells to interleukin 2. J Exp Med. 1984; 160:1147–1169. [PubMed: 6434688]
11. Phillips JH, Lanier LL. Dissection of the lymphokine-activated killer phenomenon. Relative contribution of peripheral blood natural killer cells and T lymphocytes to cytolysis. J Exp Med. 1986; 164:814–825. [PubMed: 3489062]
12. Parkhurst MR, Riley JP, Dudley ME, Rosenberg SA. Adoptive Transfer of Autologous Natural Killer Cells Leads to High Levels of Circulating Natural Killer Cells but Does Not Mediate Tumor Regression. Clin Cancer Res. 2011
13. Grabstein KH, Eisenman J, Shanebeck K, Rauch C, Srinivasan S, Fung V, et al. Cloning of a T cell growth factor that interacts with the beta chain of the interleukin-2 receptor. Science. 1994; 264:965–968. [PubMed: 8178155]
14. Carson WE, Giri JG, Lindemann MJ, Linett ML, Ahdieh M, Paxton R, et al. Interleukin (IL) 15 is a novel cytokine that activates human natural killer cells via components of the IL-2 receptor. J Exp Med. 1994; 180:1395–1403. [PubMed: 7523571]
15. Gamero AM, Ussery D, Reintgen DS, Puleo CA, Djeu JY. Interleukin 15 induction of lymphokine-activated killer cell function against autologous tumor cells in melanoma patient lymphocytes by a CD18-dependent, perforin-related mechanism. Cancer Res. 1995; 55:4988–4994. [PubMed: 7585540]
16. Koka R, Burkett PR, Chien M, Chai S, Chan F, Lodolce JP, et al. Interleukin (IL)-15R[alpha]-deficient natural killer cells survive in normal but not IL-15R[alpha]-deficient mice. J Exp Med. 2003; 197:977–984. [PubMed: 12695489]
17. Suzuki K, Nakazato H, Matsui H, Hasumi M, Shibata Y, Ito K, et al. NK cell-mediated anti-tumor immune response to human prostate cancer cell, PC-3: immunogene therapy using a highly secretable form of interleukin-15 gene transfer. J Leukoc Biol. 2001; 69:531–537. [PubMed: 11310838]
18. Kobayashi H, Dubois S, Sato N, Sabzevari H, Sakai Y, Waldmann TA, et al. Role of trans-cellular IL-15 presentation in the activation of NK cell-mediated killing, which leads to enhanced tumor immunosurveillance. Blood. 2005; 105:721–727. [PubMed: 15367431]
19. Lin CY, Chuang TF, Liao KW, Huang YJ, Pai CC, Chu RM. Combined immunogene therapy of IL-6 and IL-15 enhances anti-tumor activity through augmented NK cytotoxicity. Cancer Lett. 2008; 272:285–295. [PubMed: 18760876]
20. Waldmann TA. The biology of interleukin-2 and interleukin-15: implications for cancer therapy and vaccine design. Nat Rev Immunol. 2006; 6:595–601. [PubMed: 16868550]
21. Tasaki K, Yoshida Y, Miyauchi M, Maeda T, Takenaga K, Kouzu T, et al. Transduction of murine colon carcinoma cells with interleukin-15 gene induces antitumor effects in immunocompetent and immunocompromised hosts. Cancer Gene Ther. 2000; 7:255–261. [PubMed: 10770634]
22. Hazama S, Noma T, Wang F, Iizuka N, Ogura Y, Yoshimura K, et al. Tumour cells engineered to secrete interleukin-15 augment anti-tumour immune responses in vivo. Br J Cancer. 1999; 80:1420–1426. [PubMed: 10424745]
23. Yajima T, Nishimura H, Wajjwalku W, Harada M, Kuwano H, Yoshikai Y. Overexpression of interleukin-15 in vivo enhances antitumor activity against MHC class I-negative and -positive malignant melanoma through augmented NK activity and cytotoxic T-cell response. Int J Cancer. 2002; 99:573–578. [PubMed: 11992548]
24. Meazza R, Lollini PL, Nanni P, De Giovanni C, Gaggero A, Comes A, et al. Gene transfer of a secretable form of IL-15 in murine adenocarcinoma cells: effects on tumorigenicity, metastatic potential and immune response. Int J Cancer. 2000; 87:574–581. [PubMed: 10918200]

25. Bessard A, Sole V, Bouchaud G, Quemener A, Jacques Y. High antitumor activity of RLI, an interleukin-15 (IL-15)-IL-15 receptor alpha fusion protein, in metastatic melanoma and colorectal cancer. Mol Cancer Ther. 2009; 8:2736–2745. [PubMed: 19723883]
26. Stoklasek TA, Schluns KS, Lefrancois L. Combined IL-15/IL-15Ralpha immunotherapy maximizes IL-15 activity in vivo. J Immunol. 2006; 177:6072–6080. [PubMed: 17056533]
27. Dubois S, Patel HJ, Zhang M, Waldmann TA, Muller JR. Preassociation of IL-15 with IL-15Ralpha-IgG1-Fc enhances its activity on proliferation of NK and CD8+/CD44high T cells and its antitumor action. J Immunol. 2008; 180:2099–2106. [PubMed: 18250415]
28. Epardaud M, Elpek KG, Rubinstein MP, Yonekura AR, Bellemare-Pelletier A, Bronson R, et al. Interleukin-15/interleukin-15R alpha complexes promote destruction of established tumors by reviving tumor-resident CD8+ T cells. Cancer Res. 2008; 68:2972–2983. [PubMed: 18413767]
29. DePaolo RW, Abadie V, Tang F, Fehlner-Peach H, Hall JA, Wang W, et al. Co-adjuvant effects of retinoic acid and IL-15 induce inflammatory immunity to dietary antigens. Nature. 2011; 471:220–224. [PubMed: 21307853]
30. Vugmeyster Y, Glas R, Perarnau B, Lemonnier FA, Eisen H, Ploegh H. Major histocompatibility complex (MHC) class I KbDb -/- deficient mice possess functional CD8+ T cells and natural killer cells. Proc Natl Acad Sci U S A. 1998; 95:12492–12497. [PubMed: 9770513]
31. Ward PL, Koeppen H, Hurteau T, Schreiber H. Tumor antigens defined by cloned immunological probes are highly polymorphic and are not detected on autologous normal cells. J Exp Med. 1989; 170:217–232. [PubMed: 2787379]
32. Papadimitriou JC, Drachenberg CB, Brenner DS, Newkirk C, Trump BF, Silverberg SG. "Thanatosomes": a unifying morphogenetic concept for tumor hyaline globules related to apoptosis. Hum Pathol. 2000; 31:1455–1465. [PubMed: 11150370]
33. Arina A, Murillo O, Dubrot J, Azpilikueta A, Gabari I, Perez-Gracia JL, et al. Interleukin-15 liver gene transfer increases the number and function of IKDCs and NK cells. Gene Ther. 2008; 15:473–483. [PubMed: 18273053]
34. Chiossone L, Chaix J, Fuseri N, Roth C, Vivier E, Walzer T. Maturation of mouse NK cells is a 4-stage developmental program. Blood. 2009; 113:5488–5496. [PubMed: 19234143]
35. Moffett A, Loke C. Immunology of placentation in eutherian mammals. Nat Rev Immunol. 2006; 6:584–594. [PubMed: 16868549]
36. Barber EM, Pollard JW. The uterine NK cell population requires IL-15 but these cells are not required for pregnancy nor the resolution of a Listeria monocytogenes infection. J Immunol. 2003; 171:37–46. [PubMed: 12816981]
37. Biron CA, Welsh RM. Blastogenesis of natural killer cells during viral infection in vivo. J Immunol. 1982; 129:2788–2795. [PubMed: 7142707]
38. Stewart I, Peel S. Granulated metrial gland cells at implantation sites of the pregnant mouse uterus. Anat Embryol (Berl). 1980; 160:227–238. [PubMed: 7457918]
39. Stallmach T, Ehrenstein T, Isenmann S, Muller C, Hengartner H, Kagi D. The role of perforin-expression by granular metrial gland cells in pregnancy. Eur J Immunol. 1995; 25:3342–3348. [PubMed: 8566021]
40. Fehniger TA, Shah MH, Turner MJ, VanDeusen JB, Whitman SP, Cooper MA, et al. Differential cytokine and chemokine gene expression by human NK cells following activation with IL-18 or IL-15 in combination with IL-12: implications for the innate immune response. J Immunol. 1999; 162:4511–4520. [PubMed: 10201989]
41. Brady J, Carotta S, Thong RP, Chan CJ, Hayakawa Y, Smyth MJ, et al. The interactions of multiple cytokines control NK cell maturation. J Immunol. 2010; 185:6679–6688. [PubMed: 20974986]
42. Park JY, Lee SH, Yoon SR, Park YJ, Jung H, Kim TD, et al. IL-15-induced IL-10 increases the cytolytic activity of human natural killer cells. Mol Cells. 2011; 32:265–272. [PubMed: 21809216]
43. Jain RK. Transport of molecules in the tumor interstitium: a review. Cancer Res. 1987; 47:3039–3051. [PubMed: 3555767]
44. Pegram HJ, Haynes NM, Smyth MJ, Kershaw MH, Darcy PK. Characterizing the anti-tumor function of adoptively transferred NK cells in vivo. Cancer Immunol Immunother. 2010; 59:1235–1246. [PubMed: 20376439]

45. Wilcox RA, Tamada K, Strome SE, Chen L. Signaling through NK cell-associated CD137 promotes both helper function for CD8+ cytolytic T cells and responsiveness to IL-2 but not cytolytic activity. J Immunol. 2002; 169:4230–4236. [PubMed: 12370353]

46. Spiotto MT, Rowley DA, Schreiber H. Bystander elimination of antigen loss variants in established tumors. Nat Med. 2004; 10:294–298. [PubMed: 14981514]

47. Croy BA, Esadeg S, Chantakru S, van den Heuvel M, Paffaro VA, He H, et al. Update on pathways regulating the activation of uterine Natural Killer cells, their interactions with decidual spiral arteries and homing of their precursors to the uterus. J Reprod Immunol. 2003; 59:175–191. [PubMed: 12896821]

48. Kroemer A, Xiao X, Degauque N, Edtinger K, Wei H, Demirci G, et al. The innate NK cells, allograft rejection, and a key role for IL-15. J Immunol. 2008; 180:7818–7826. [PubMed: 18523245]

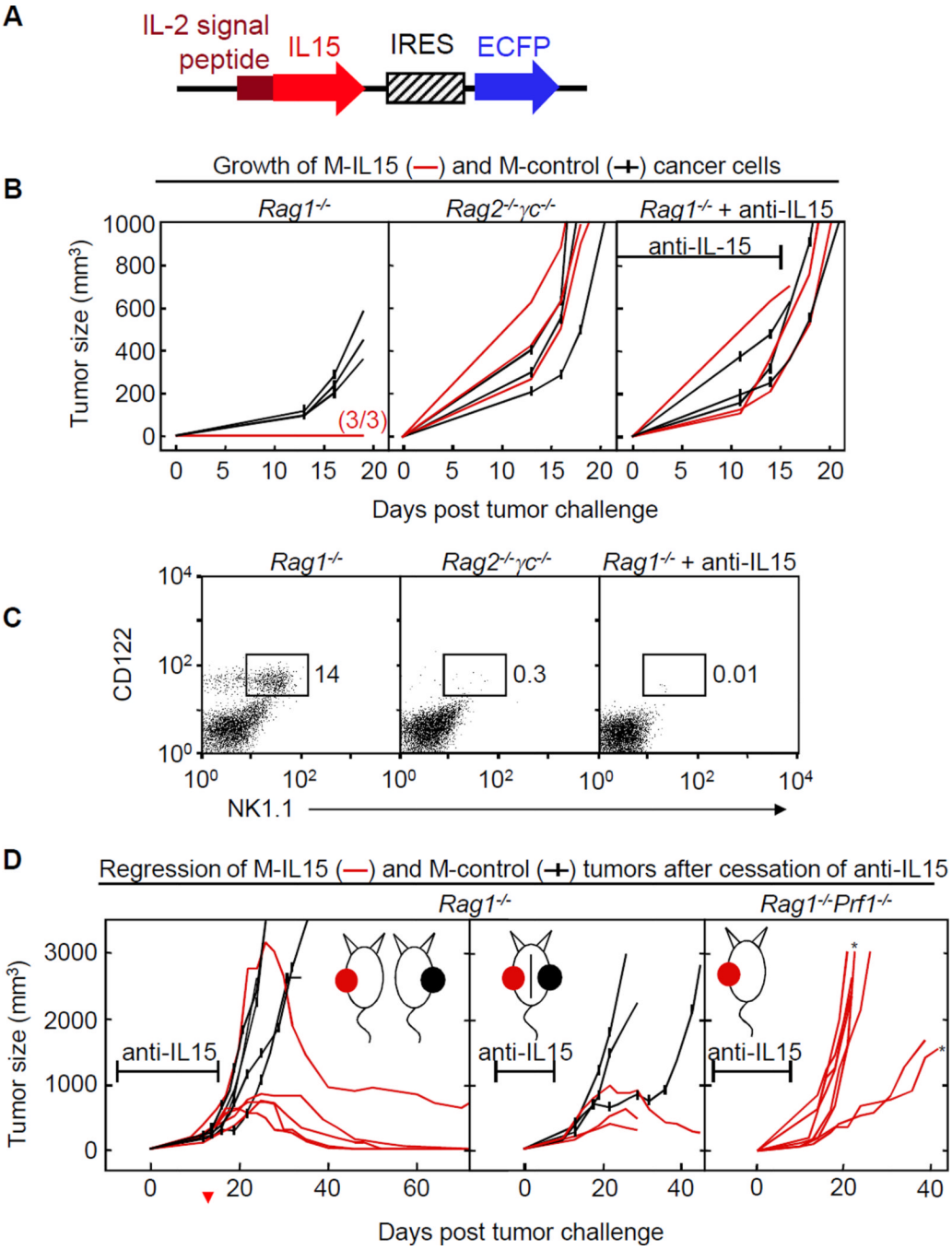

Figure 1. Local expression of IL15 causes rejection of established tumors

A) IL15 construct introduced to MC57 cells (M-IL15). **B)** Growth of M-IL15 and M-control cells in *Rag1*$^{-/-}$, *Rag2*$^{-/-}$ $\gamma c^{-/-}$ and *Rag1*$^{-/-}$ mice receiving anti-IL15 antibody. Mice were injected with either M-control (black) or M-IL15 cells (red) at day 0. Results are pooled from six experiments. **C)** Comparison of NK1.1^{+}CD122^{+} NK populations in peripheral blood of *Rag1*$^{-/-}$, *Rag2*$^{-/-}$$\gamma c^{-/-}$ and *Rag1*$^{-/-}$ mice receiving anti-IL15 antibody. **D)** Mice were given anti-IL15 antibody until tumors had formed. Data are pooled from at least two experiments for each group. Left, *Rag1*$^{-/-}$ mice were injected with M-control or M-IL15. Data of two mice from the control group are also shown in B. Middle, *Rag1*$^{-/-}$ mice were

contra-laterally injected with M-control and M-IL15. Right, *Rag1*$^{-/-}$*Prf1*$^{-/-}$ mice were injected with M-IL15. Asterisks marked mice were not given anti-IL15. The antibody marker represents the average time of anti-IL15 treatment (day -7 to day 15 for B; days −7 to 16, −7 to 8, and −7 to 7 for D left, middle and right, respectively). Each line represents an individual mouse.

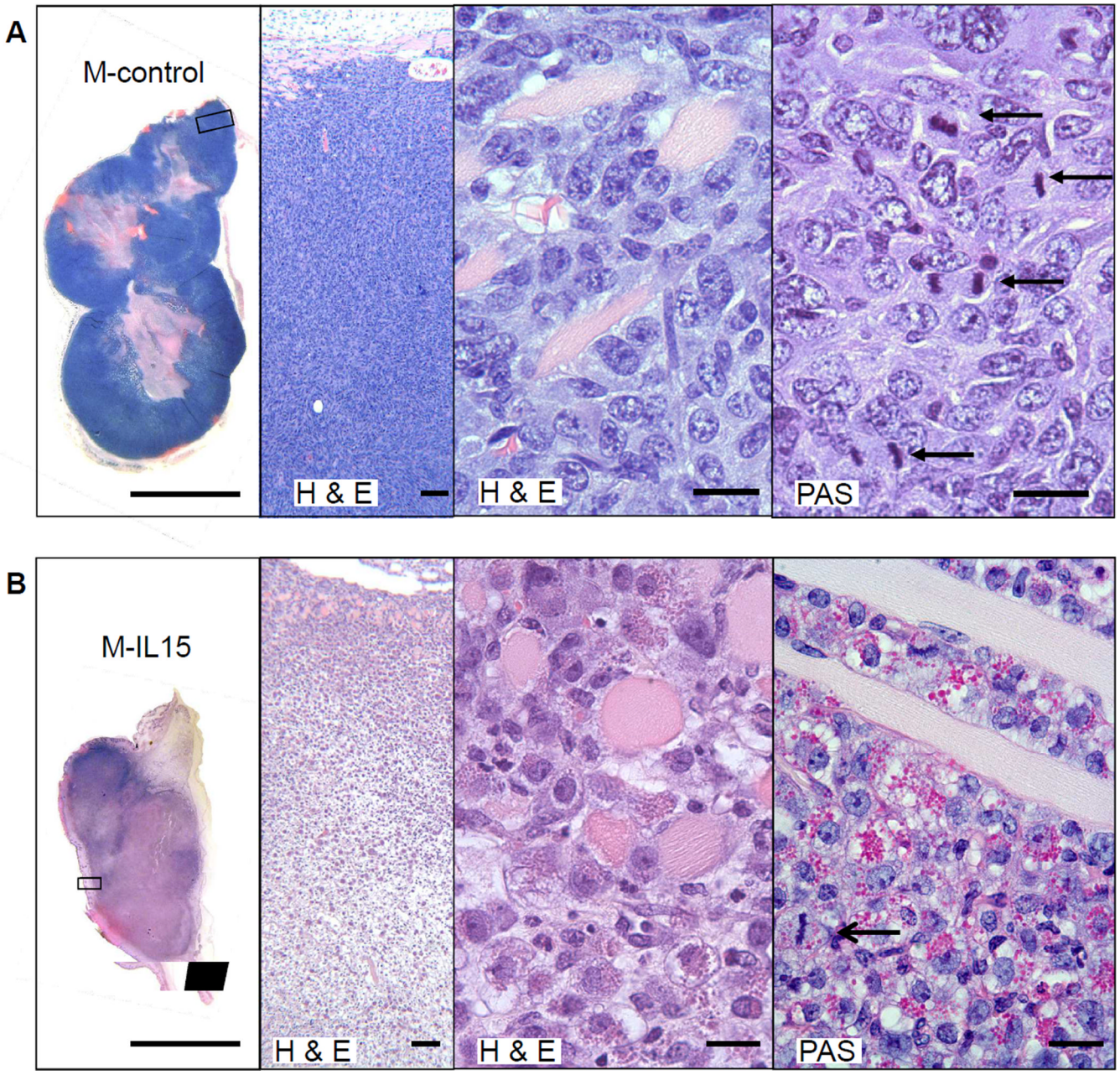

Figure 2. Proliferating PAS^{+} granular cells infiltrate M-IL15 tumors

Macroscopic and microscopic photographs of tumors grown in *Rag1*$^{-/-}$ mice given anti-IL15 and harvested at day 26, 12 days after the final antibody injection. Histological sections of tumors stained with H&E and PAS. Scale bars from left to right are 1cm, 100μm, 20μm, and 20μm. **A)** Note the thick blue outer layer of the M-control tumor that, as seen at higher resolution, is packed with viable cancer cells. The eosinophilic center of the tumor shows a relatively small necrotic tumor center. Arrows show mitotic figures in cancer cells. **B)** By contrast, the IL15-secreting tumor shows extensive necrosis. The open arrow denotes an example of repeatedly observed mitotic figures in the granulated cell indicating proliferation in the tumor.

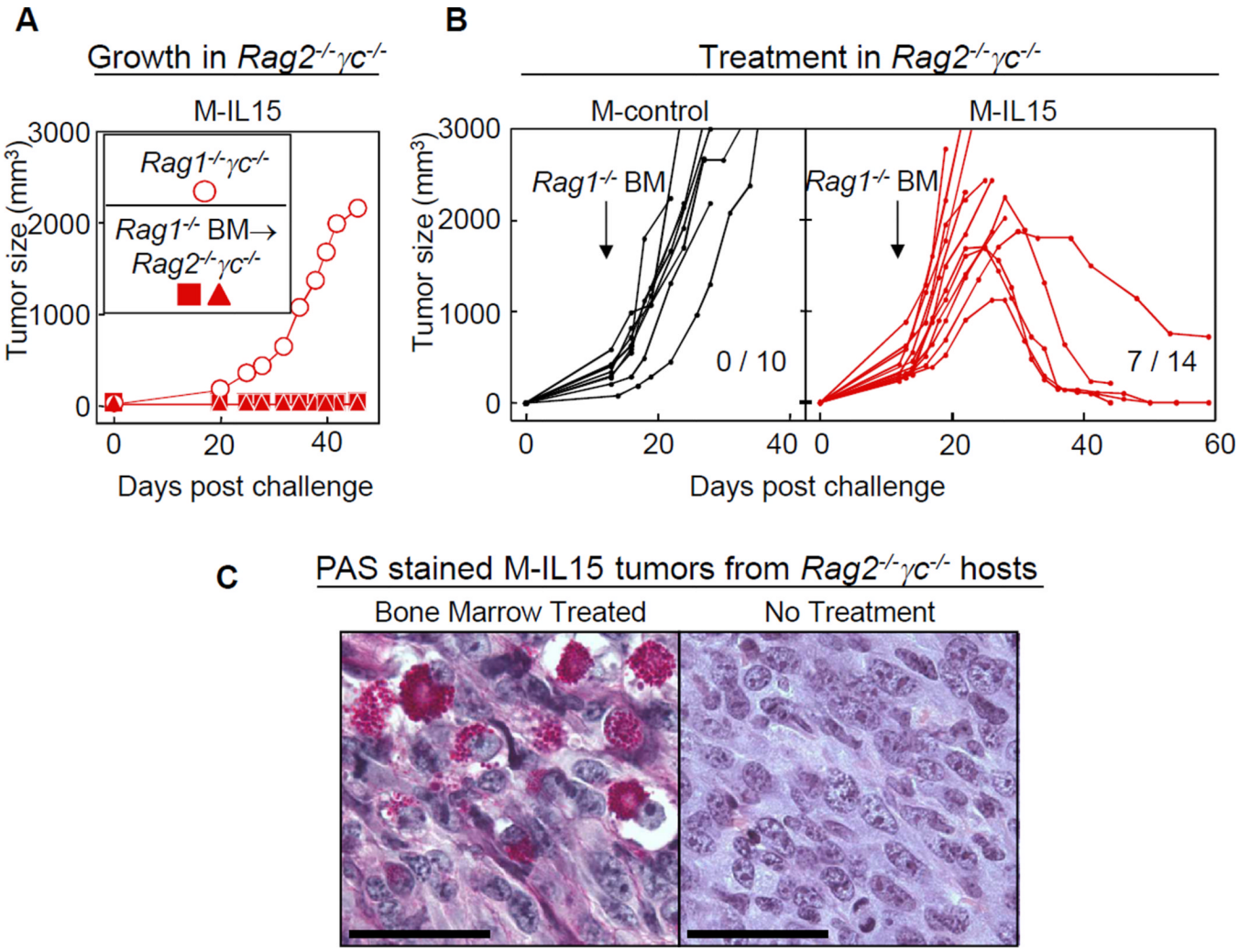

Figure 3. Adoptive transfer of *Rag1*$^{-/-}$ bone marrow cells prevents cancer development and can also eradicate established M-IL15 tumors

A) Reconstitution of *Rag2*$^{-/-}$ $\gamma c^{-/-}$ mice with *Rag1*$^{-/-}$ bone marrow renders them resistant to challenge with IL15-secreting cancer cells. Recipient *Rag2*$^{-/-}$ $\gamma c^{-/-}$ mice received bone marrow from *Rag1*$^{-/-}$ donors two months before challenge with M-IL15 cells. Each symbol represents an individual mouse. Data are representative of two individual experiments. **B)** Adoptive transfer of *Rag1*$^{-/-}$ bone marrow can eradicate established M-IL15 tumors in *Rag2*$^{-/-}$$\gamma c^{-/-}$ mice. *Rag2*$^{-/-}$$\gamma c^{-/-}$ mice were challenged *s.c.* with M-control (black) or M-IL15 (red) cells. Mice were injected with *Rag1*$^{-/-}$ bone marrow cells *i.v.* at day 12–14, depending on the size of the tumor. Tumors reached an average size of 423 mm^3 for M-IL15 tumors and 339 mm^3 for M-control tumors at the time of treatment. Data are pooled from at least four independent experiments for each group. Numbers indicate eradicated tumors per number of tumors treated ($p<0.02$). Each line represents an individual mouse. **C)** Dense infiltrates of leukocytes resembling uterine NK cells are found in M-IL15 tumors in *Rag2*$^{-/-}$$\gamma c^{-/-}$ mice that received *Rag1*$^{-/-}$ BM. M-IL15 tumor sections from a *Rag2*$^{-/-}$$\gamma c^{-/-}$ mouse 14 days after treatment with *Rag1*$^{-/-}$ BM were stained with PAS & diastase. For comparison, an untreated M-IL15 tumor grown in a *Rag2*$^{-/-}$$\gamma c^{-/-}$ mouse is shown. Data are representative of two individual mice. Scale bars are 100 μm.

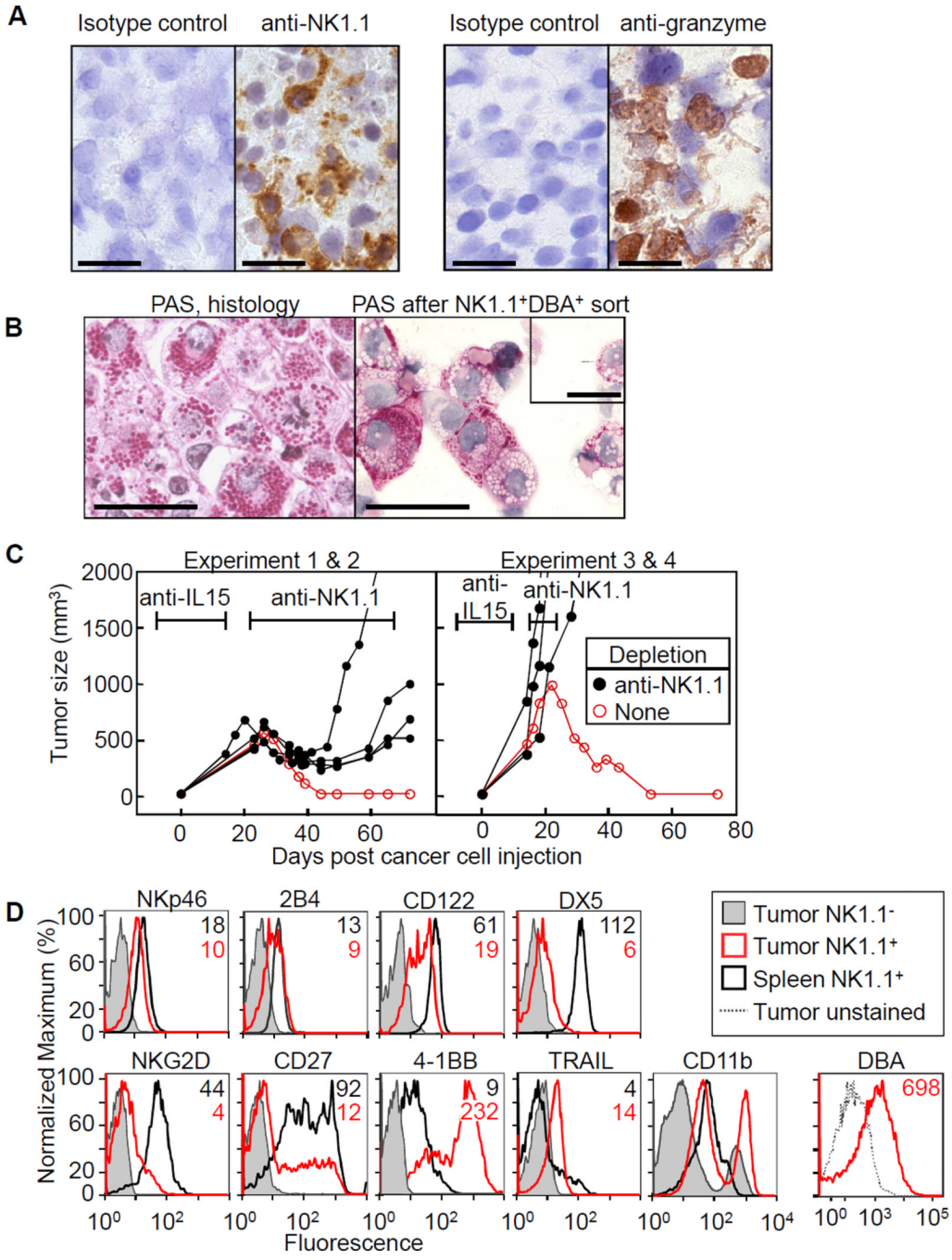

Figure 4. NK cells are required for rejection of M-IL15 tumors in *Rag1*$^{-/-}$ mice

A) Immunohistochemistry with anti-NK1.1, anti-granzyme B and respective isotype controls, of an M-IL15 tumor initially grown under anti-IL15 antibody in a *Rag1*$^{-/-}$ mouse. Scale bars are 20μm. **B)** PAS stain of sorted NK1.1^{+} cells from M-IL15 tumors and a formalin-fixed sample of the same tumor. Scale bars are 50μm. Inset, an embryonic day 10 uterine NK cell stained with PAS (scale bar is 20μm). **C)** *Rag1*$^{-/-}$ mice were given anti-IL15 beginning one week before cancer cell injection until one (right panel) to two (left panel) weeks after, at which point anti-NK1.1 antibody was given twice weekly (black lines) or no further treatment was given (red lines). At day 0 mice were injected with M-IL15 cells. Each

line represents an individual mouse. The antibody markers represent the average time of treatment: left, anti-IL15 (days −7–14) and anti-NK1.1 (beginning at day 22); right, anti-IL15 (days −7–10) and anti-NK1.1 (beginning at day 15). **D)** M-IL15 tumors were grown in a *Rag1*$^{-/-}$*Prf1*$^{-/-}$ mouse (tumor for CD11b-staining was grown in *Rag1*$^{-/-}$ mouse and the tumor was excised on day 60 after last anti-IL15 dose). Spleen (black) and tumor (red) were harvested and stained with anti-NK1.1 and antibodies indicated. The NK1.1^{-} population is shown for comparison (shaded). Data are representative of at least two independent experiments. Since no morphological differences were seen between densely granulated NK cells in perforin-deficient and sufficient mice (see Fig. 5), we believe the flow data shown here is representative for both settings.

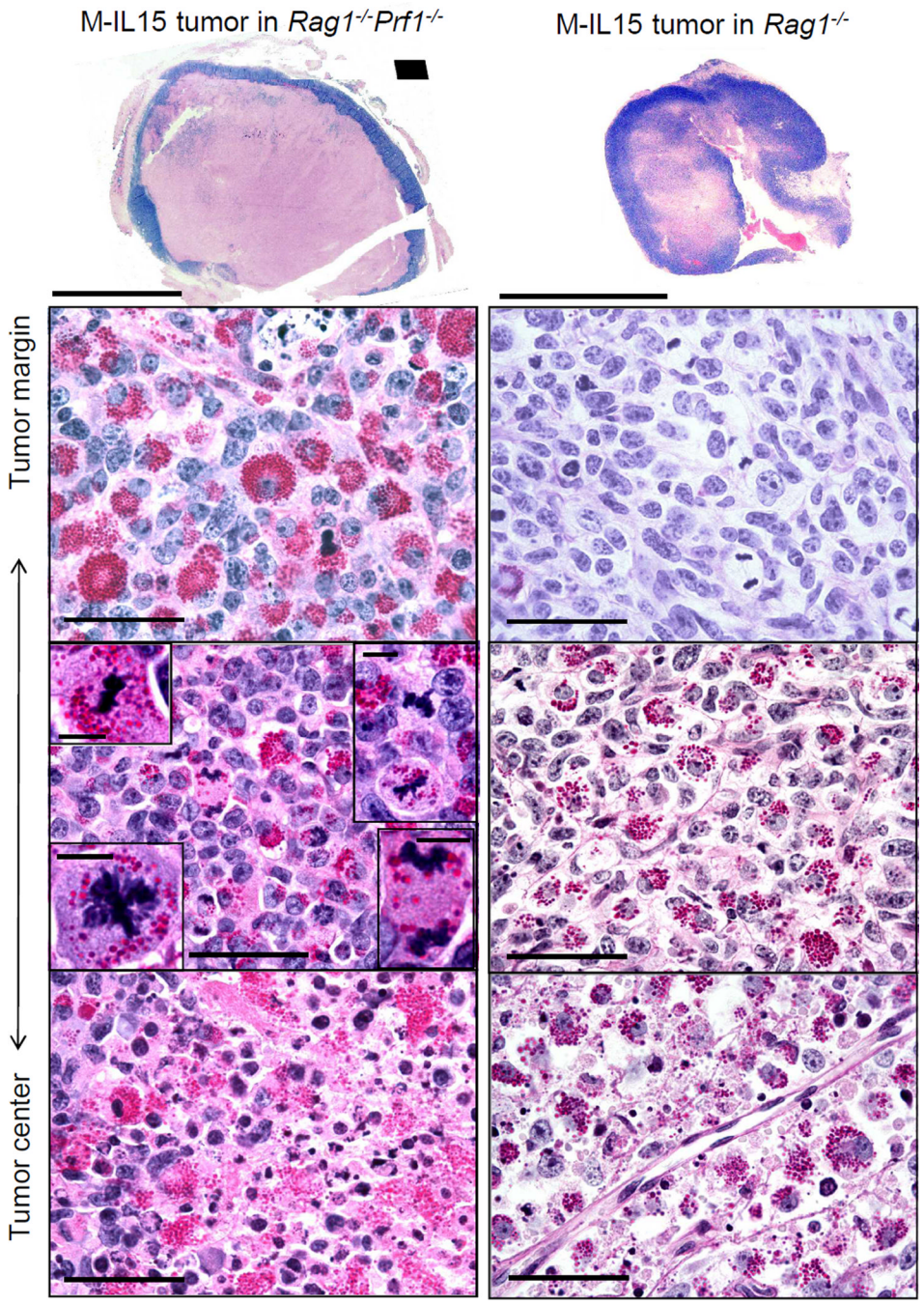

Figure 5. Eradication depends on eliminating cancer at the tumor rim

Macroscopic and microscopic photographs of tumors grown in anti-IL15 treated mice. Left, a *Rag1*$^{-/-}$*Prf1*$^{-/-}$ mouse 31 days after M-IL15 injection and 14 days after the final anti-IL15 injection. Right, a *Rag1*$^{-/-}$ mouse at 16 days after M-IL15 injection and 2 days after final anti-IL15 injection. Tumor sections were stained with PAS & diastase. Scale bars for macroscopic photographs are 1cm. Microscopic photographs were taken in various regions of the tumors, as depicted on the left. Scale bars for microscopic photographs are 100μm. Insets show mitotic granular NK cells (scale bars are 10μm).

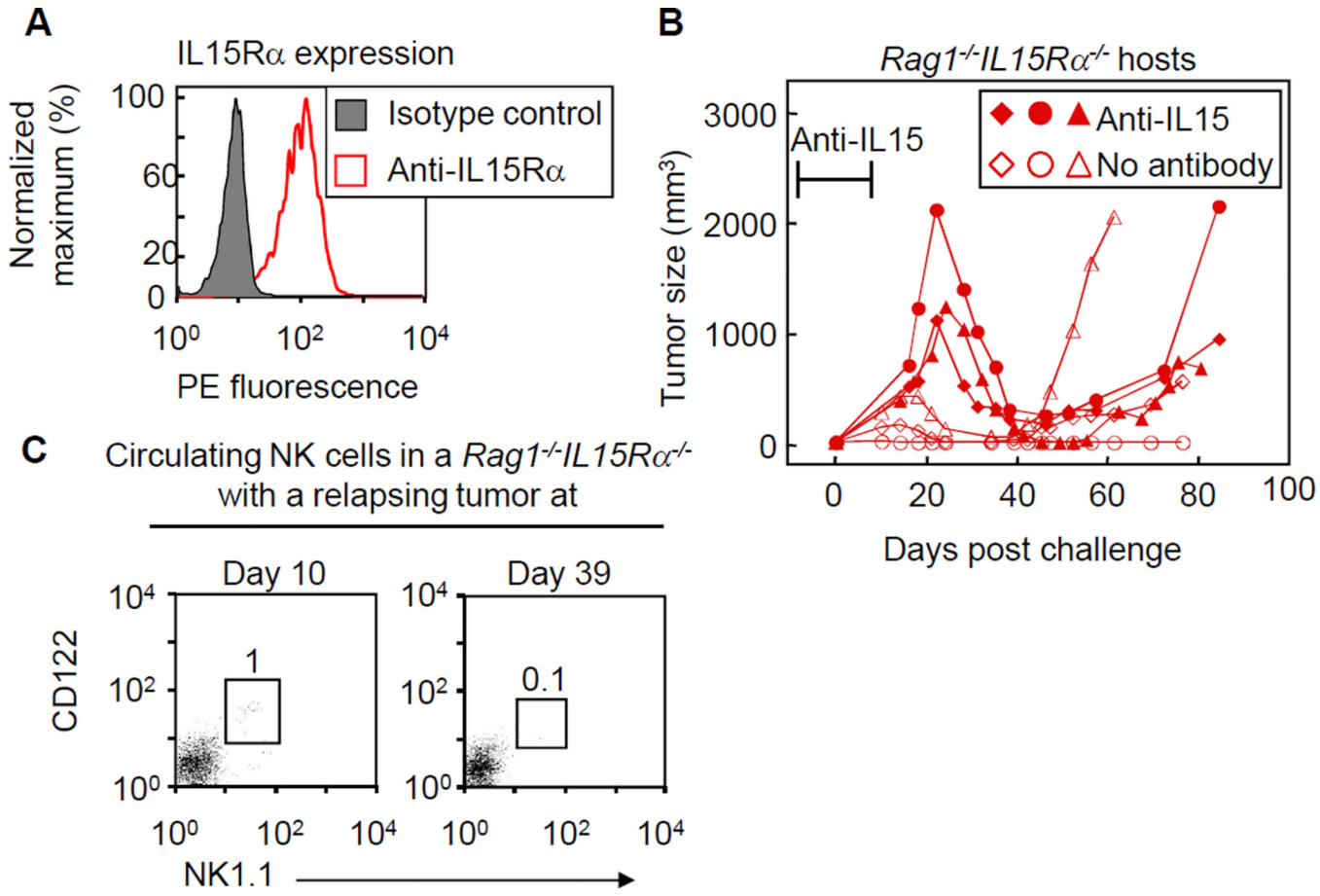

Figure 6. IL15Rα expression by stroma is required for complete tumor elimination

A) MC57 cells were stained with anti-IL15Rα antibody. **B)** *Rag1*$^{-/-}$*IL15Rα*$^{-/-}$ mice, either untreated or treated early with anti-IL15 antibody, were challenged with M-IL15 cells and tumor size was monitored. Each line represents an individual mouse. Data are pooled from three independent experiments. The antibody markers represent the average time of anti-IL15 (days −7–7). **C)** Peripheral blood from *Rag1*$^{-/-}$*IL15Rα*$^{-/-}$ mouse (not treated with anti-IL15 antibody) bearing a relapsing tumor was stained with anti-NK1.1 and anti-CD122 and analyzed by flow cytometry. Number indicates the percentage of gated cells.

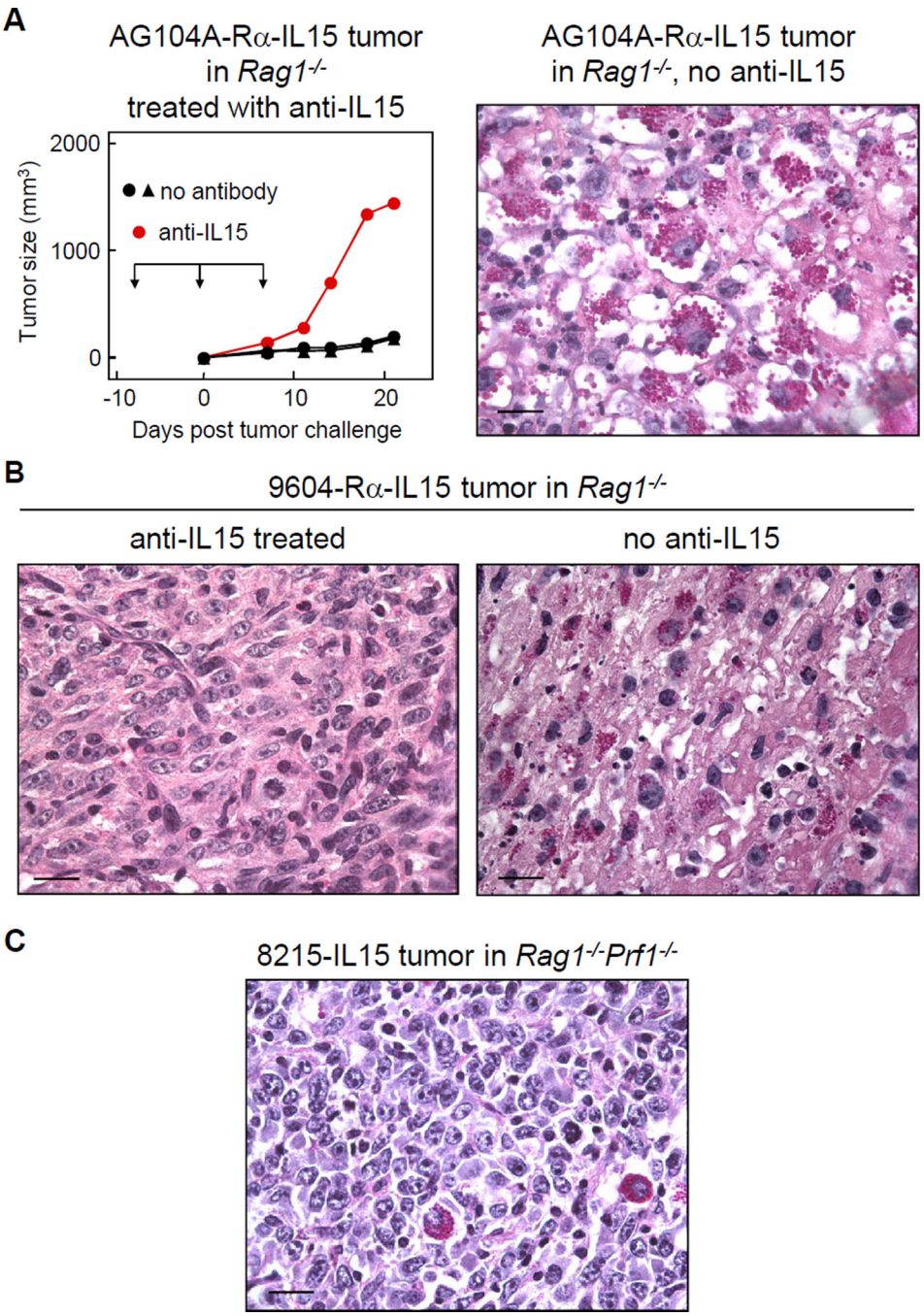

Figure 7. Densely granulated NK cells are induced by different cancer lines overexpressing IL15

A) AG104A-Rα-IL15 cancer cells grow out in *Rag1*$^{-/-}$ mice treated with anti-IL15 antibody. The tumor was not rejected after cessation of antibody treatment (day 7) due to the selection of an IL15-loss variant (data not shown). Microscopic photograph of a 21 day-old AG104A-Rα-IL15 tumor in a non-antibody-treated Rag$^{-/-}$ mouse shows cancer cell destruction and densely granulated NK cells. **B)** 9604-Rα-IL15 cancer cells form a viable tumor with no granulated NK cell infiltration in an anti-IL15-treated *Rag1*$^{-/-}$ mouse (left), while the lesion in the non-treated mouse showed infiltration of densely granulated NK cells and cancer cell death (right). Both mice were sacrificed on day 18 after cancer cell injection.

C) The IL15Rα-deficient cancer line 8215-IL15 develops viable tumors in *Rag1*$^{-/-}$*Prf1*$^{-/-}$ mice. Only very few granulated NK cells can be detected of day 16 after cancer cell injection. All tumor sections were stained with PAS & diastase. Scale bars are 20μm.